

Robust Sahel drought due to the Interdecadal Pacific Oscillation in CMIP5 simulations.

Julián Villamayor¹ and Elsa Mohino²

Affiliation:

^{1,2}Departamento de Física de la Tierra, Astronomía y Astrofísica I, Universidad

Complutense de Madrid, Madrid, Spain.

Contact:

¹Av. Complutense s/n, 28040 Madrid, Spain. julian.villamayor@fis.ucm.es

²Av. Complutense s/n, 28040 Madrid, Spain. emohino@fis.ucm.es

1. Information relating to the Monte Carlo-based test used to determine the significance of the model-mean regression maps:

A Monte Carlo test is used to test the regression maps averaged across the 17 models by comparing the averaged correlation against a probability density function. This density function is constructed from mean correlations out of 17 pairs of random time series. The length of these time series is the number of years times the number of realizations available of each of the 17 models (see Table S1), since we analyze the data of the models with several realizations available concatenated in time. For each correlated pair, one random time series is 13-year lowpass-filtered and the other is not, similarly to what we do when regress the IPO filtered indices onto the unfiltered anomaly fields to

feature the spatial patterns. We repeat the process 1000 times to build the probability density function against which the original mean regression is compared.

2. Supplementary table and figures that may be useful to better follow the article:

		piControl	historical		rcp8.5	
		#yrs	#yrs	#rea	#yrs	#rea
1	bcc-csm1-1	500	163*	3	95	1
2	CanESM2	996	156	5	95	5
3	CCSM4	501	156	6	95	6
4	CNRM-CM5	850	156	10	95	5
5	CSIRO-Mk3-6-0	500	156	10	95	10
6	FGOALS-g2	700	156	4	95	1
7	GISS-E2-H	540	156	5	95	5
8	GISS-E2-R	550	156	6	95	5
9	HadGEM2-CC	240	145**	1	94***	3
10	HadGEM2-ES	575	145**	5	95	4
11	inmcm4	500	156	1	95	1
12	IPSL-CM5A-LR	1000	156	6	95	4
13	MIROC5	670	163*	5	95	3
14	MIROC-ESM-CHEM	255	156	1	95	1
15	MPI-ESM-LR	1000	156	3	95	3
16	MRI-CGCM3	500	156	5	95	1
17	NorESM1-M	501	156	3	95	1

Table S1. List of CMIP5 models analyzed, number of years (#yrs) and realizations (#rea) of each simulation. The historical experiment are simulations of the period 1850-2005 (exceptions are 1850-2012 (*) and 1860-2004 (**)). The rcp8.5 simulation period is 2006-2100 (exception is 2006-2099(***)). All data are available at <http://pcmdi9.llnl.gov>.

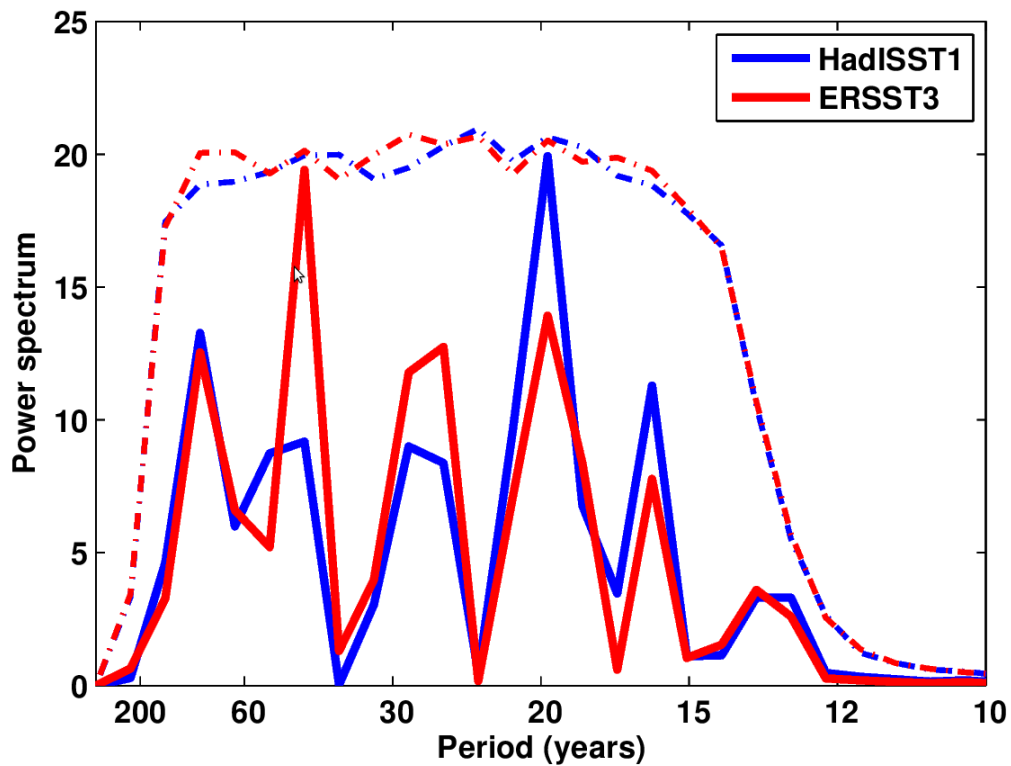


Figure S1. Power spectrum of the Fourier transform of the detrended IPO indices from observations. Dashed lines indicate the 95% confidence level following a Monte Carlo-based test in which a probability density is built from the Fourier spectrum of 13-year lowpass-filtered and detrended white noise time series.

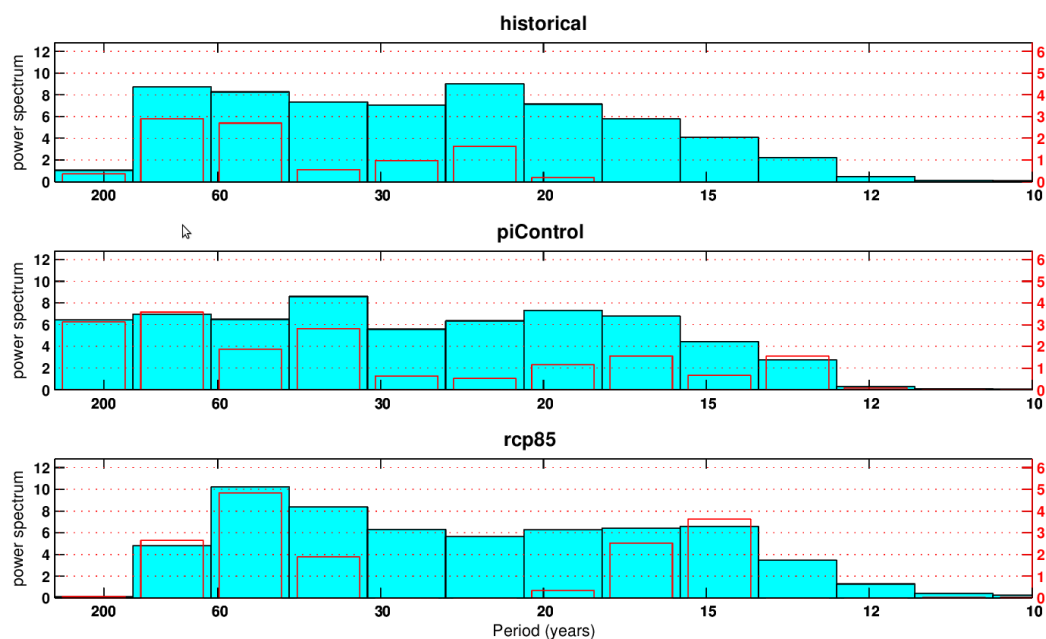
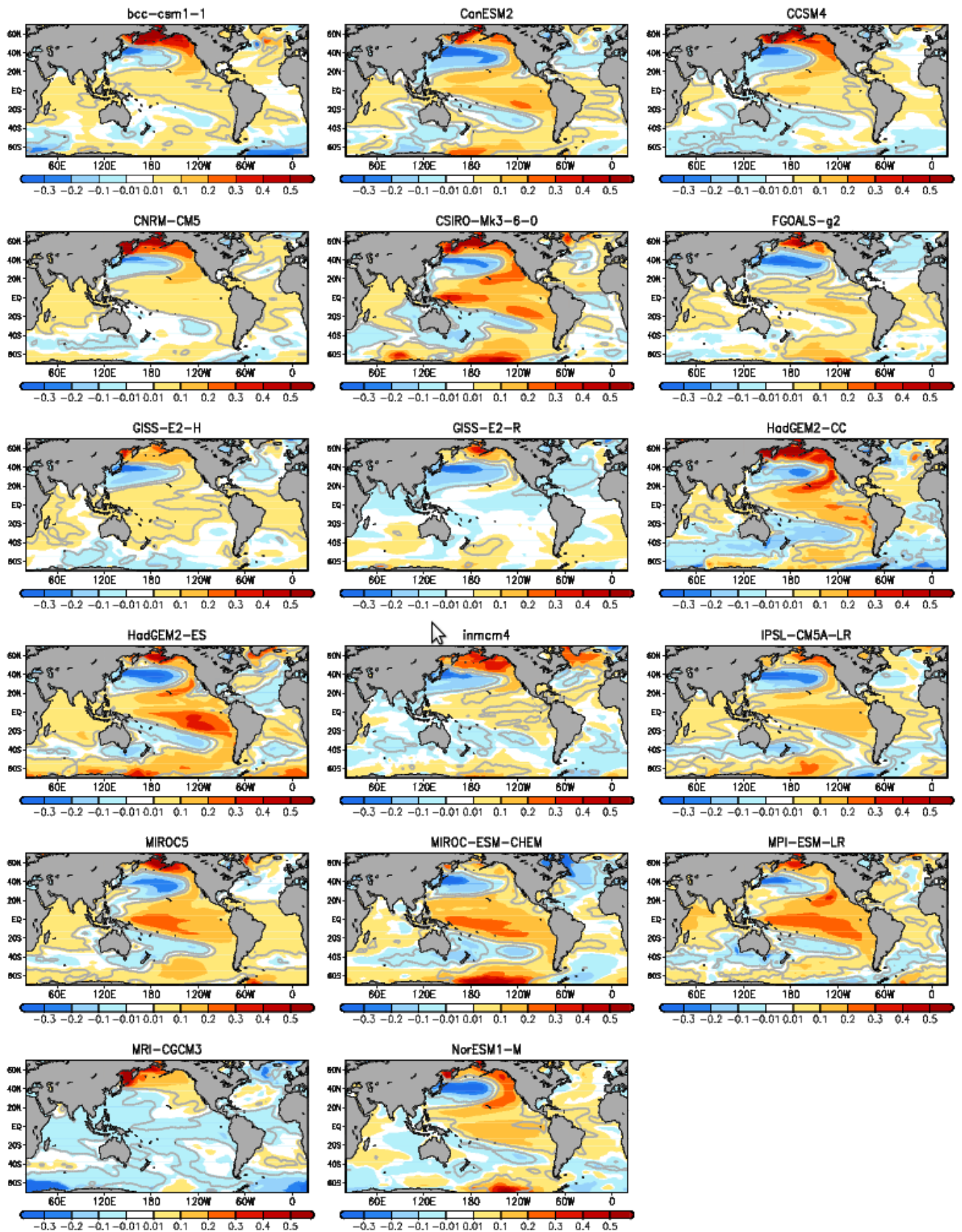


Figure S2. Model-mean power spectra of the Fourier transform of the detrended IPO indices (blue bars) of the historical (top), piControl (middle) and rcp8.5 simulations (bottom). Red bars indicate the power spectra averaged over the 17 models but taking into account only 95% significant peaks for each of them. The statistical significance for each model's IPO is obtained following a Monte Carlo-based test in which a probability density function is built from the Fourier spectrum of 13-year lowpass-filtered and detrended white noise time series with the same time length as the simulation and averaged across the number of ensemble members in cases where more than one realization is available.

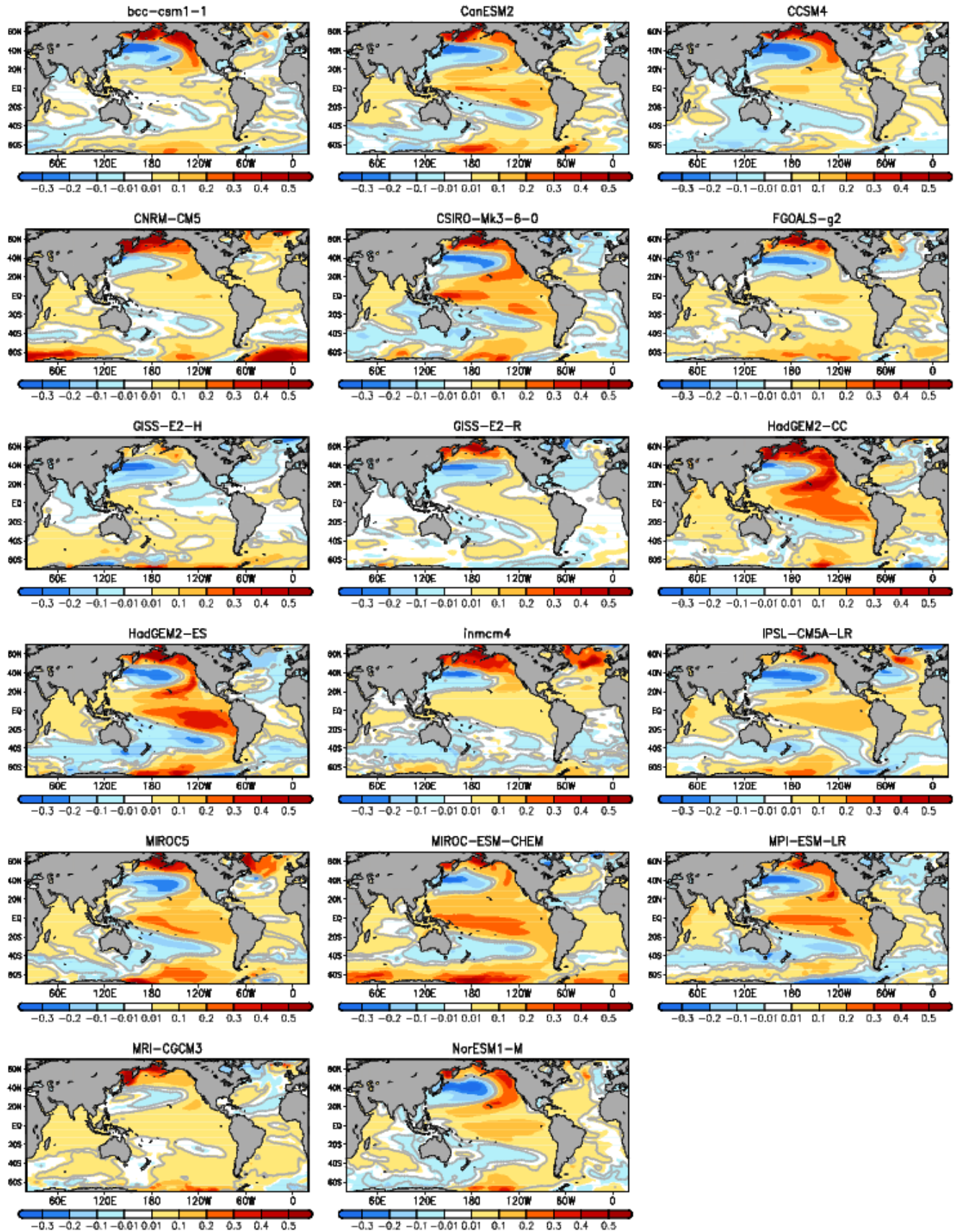


59 **Figure S3.** Single models IPO SST patterns from historical simulations defined as the
60 regression of the SSTA onto the standardized IPO index (units are K per standard

61 deviation). Grey contours indicate the regions where the correlation is significant with a
62 significance level of 0.05 (from a t-test).

63

64



65 **Figure S4.** Single models IPO SST patterns from piControl simulations defined as the
66 regression of the SSTA onto the standardized IPO index (units are K per standard

deviation). Grey contours indicate the regions where the correlation is significant with a significance level of 0.05 (from a t-test).

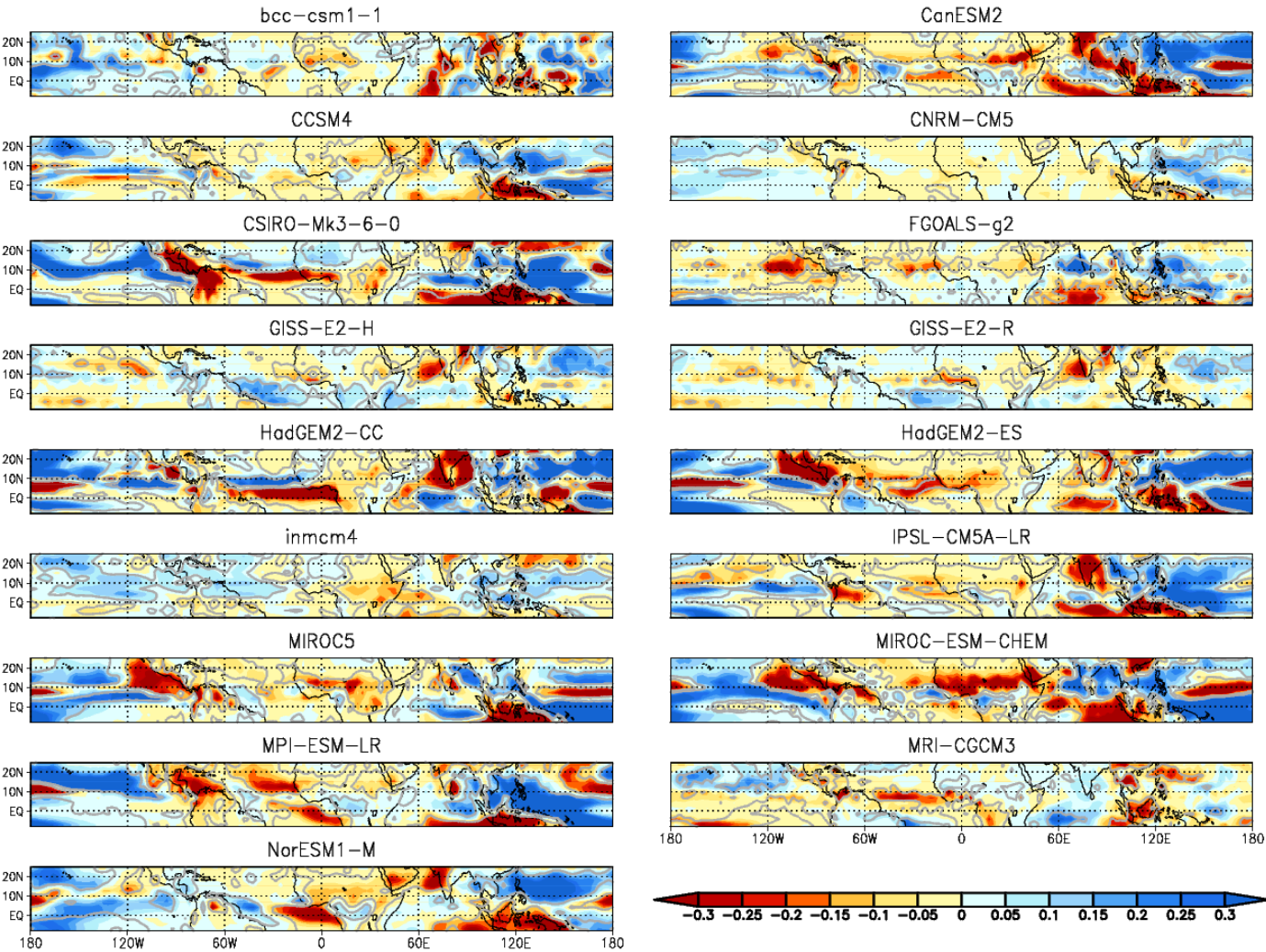
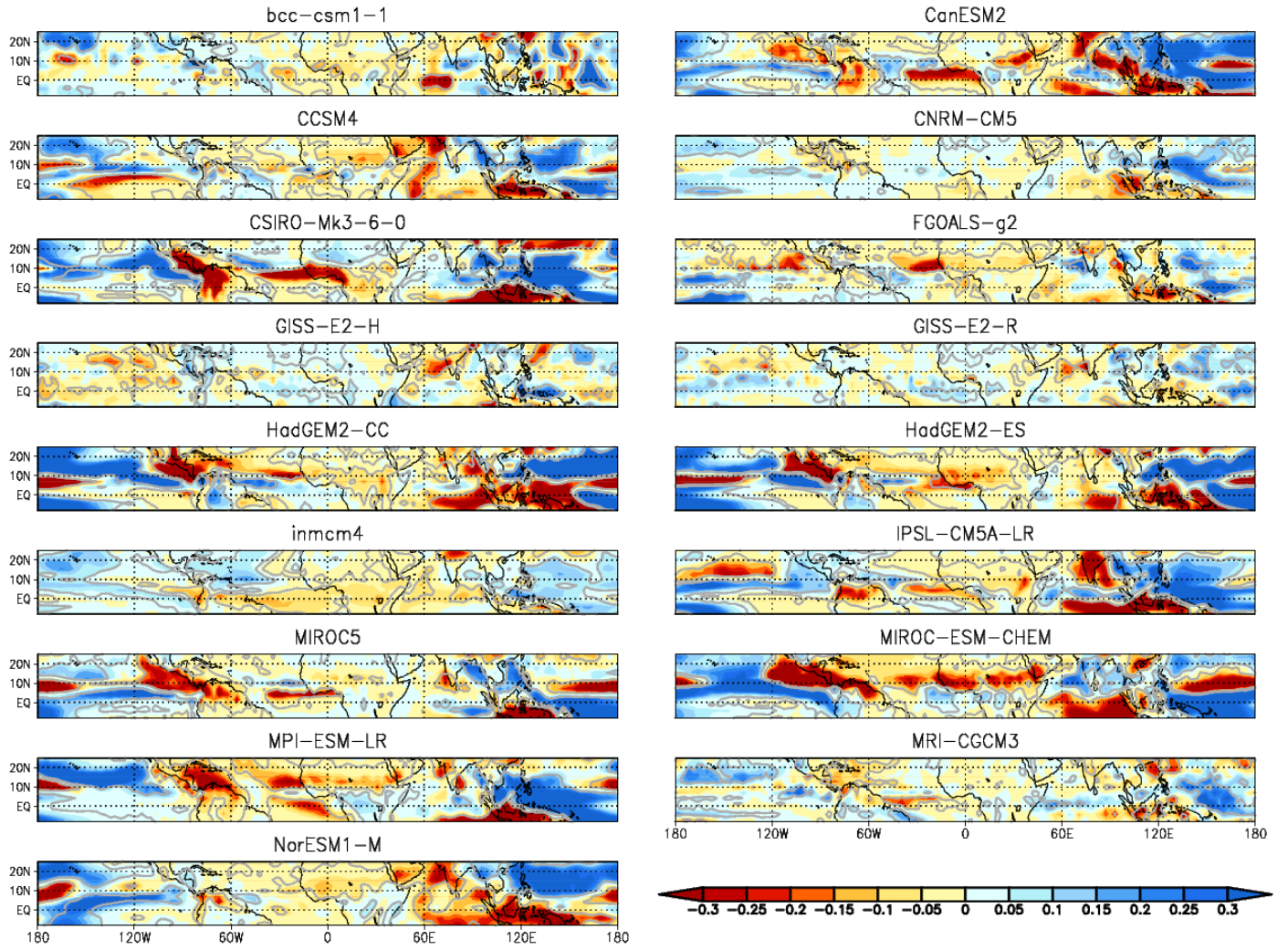


Figure S5. Single models regression maps of JAS precipitation anomalies onto the standardized IPO index (mm/day per std. dev.) from historical simulations. Grey contours indicate the regions where the correlation is significant with a significance level of 0.05 (from a t-test).



76 **Figure S6.** Single models regression maps of JAS precipitation anomalies onto the
 77 standardized IPO index (mm/day per std. dev.) from piControl simulations. Grey
 78 contours indicate the regions where the correlation is significant with a significance
 79 level of 0.05 (from a t-test).

80

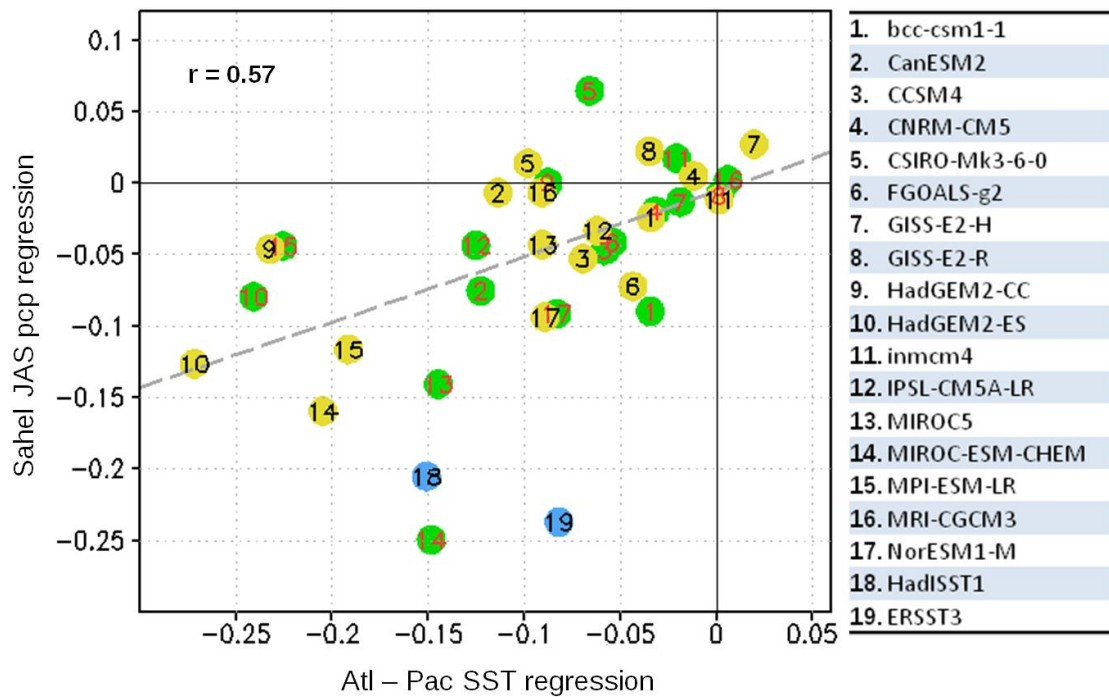


Figure S7. Scatter plot of the regression coefficient of precipitation anomaly over Sahel (between 17°-10°N and 10°W-10°E, see box in Figure 2b) (units are mm/day per std. dev.), and the SSTA difference between the Tropical Atlantic coastal region next to West Africa (25°-15°N and 30°-18°W, see box over the Tropical Atlantic in Figure 2a) and the Tropical Pacific (15°N-15°S and 180°-95°W, see box over the Tropical Pacific in Figure 2a) SSTA (units are K per std. dev.). The regression line fitted to all the points has a correlation coefficient $R=0.57$. Numbers from 1 to 17 correspond to single models; 18 and 19 correspond to observations.

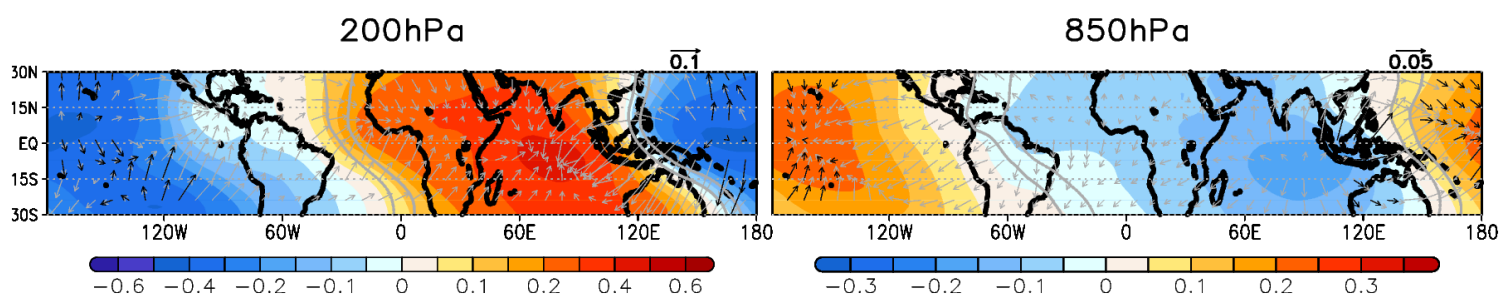
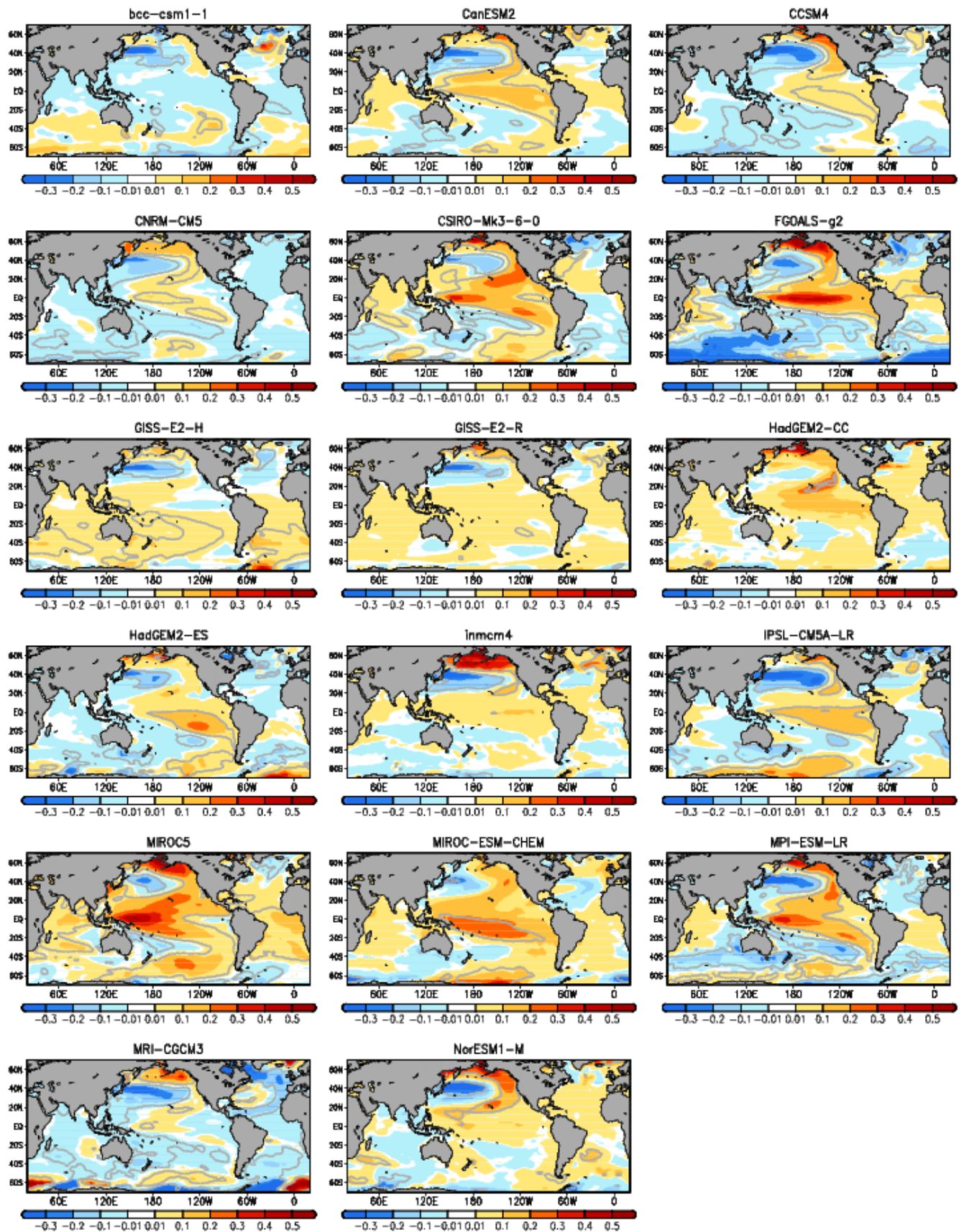


Figure S8. Averaged regression in the rcp8.5 simulation of the JAS anomaly of velocity potential at 200 hPa and 850 hPa onto the standardized IPO index ($10^6 \text{ m}^2/\text{s}$ per std. dev.). Divergent wind derived from this pattern is represented by black vectors at points where the sign of the regression coefficient of the velocity potential coincides in at least 15 out of the 17 models analyzed and by gray vectors at the rest of the points. Grey contours indicate the regions where the averaged correlation is significant at $\alpha=0.05$ (using a Monte Carlo-based test, see details in the supplementary material).



101 **Figure S9.** Single models IPO SST patterns from rcp8.5 simulations defined as the
 102 regression of the SSTA onto the standardized IPO index (units are K per standard

deviation). Grey contours indicate the regions where the correlation is significant with a significance level of 0.05 (from a t-test).

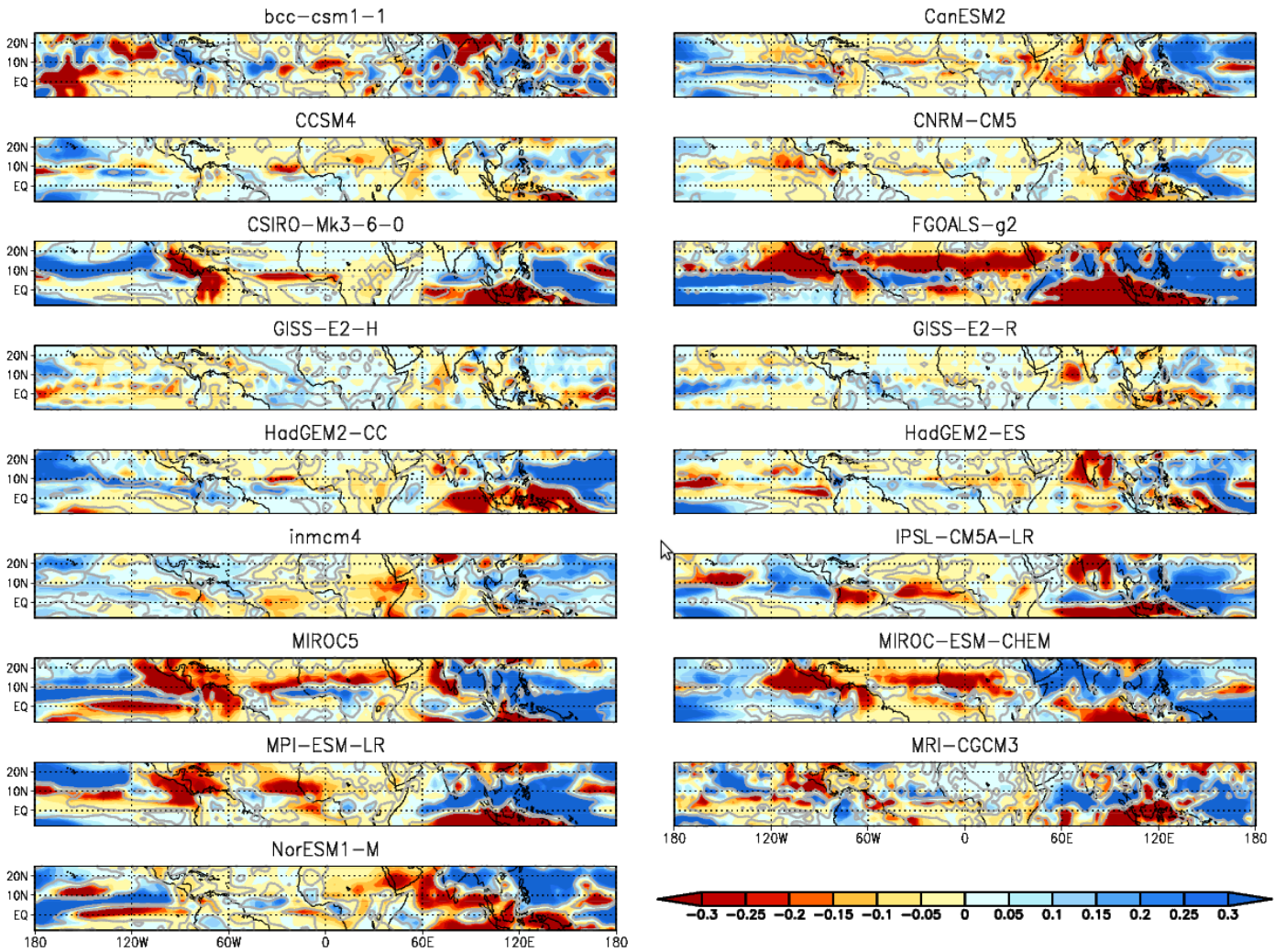


Figure S10. Single models regression maps of JAS precipitation anomalies onto the standardized IPO index (mm/day per std. dev.) from rcp8.5 simulations. Grey contours indicate the regions where the correlation is significant with a significance level of 0.05 (from a t-test).